ELSEVIER

Composites: Part B 30 (1999) 523–534

composites
Part B: engineering

Design and manufacturing considerations for ply drops in composite structures

D.S. Cairns*, J.F. Mandell, M.E. Scott, J.Z. Maccagnano

Montana State University, DOE EPSCoR Wind Energy Cluster, Bozeman, MT 59717, USA

Received 17 February 1998; accepted 28 May 1998

Abstract

Thickness variations are required to optimize the design of modern laminated composite structures. These thickness variations are accomplished by dropping plies along the length to match varying in-plane and bending loads. This results in a structure which is matched to stiffness and loading requirements. Unfortunately, these ply drops produce internal and local stress concentrations as a consequence of geometric discontinuities and shear lag. In this study, we explore various factors for design of composite structures with ply drops. These factors include: thicknesses, ply stacking sequences, ply drop geometries and manufacturing considerations. In addition, fatigue loading is considered with respect to delamination initiation and growth. A strong sensitivity to the position and the manufacturing details of ply drops is shown for fatigue damage initiation and growth. All studies were conducted on a low-cost E-glass/polyester composite system. The results indicate that it will be difficult to completely suppress damage and delamination initiation in service. However, it was found that, in many cases, there is a threshold loading under which there is little growth after initiation is noted. Factors affecting this threshold are analyzed via the virtual crack closure method in Finite Element Analysis and verified experimentally. Design rules for ply dropping are presented on the basis of these results.

Keywords: Ply-drops; B. Delamination; Strain energy release rate; B. Fracture; B. Fatigue

1. Introduction

Ply drops in composite materials are a relevant design consideration in many structures, especially those with varying loads throughout the structure. As an example, each ply in a composite laminate without bending needs to carry the same amount of strain when a ply is dropped. There is a reduction in area that places the thinner section under a higher stress, transitioning via shear lag. The ply drop introduces a stress concentration, causing a crack to form and propagate along the layer that forms the ply drop.

There are three possibilities for crack growth:

1. The driving force is high enough to propagate the crack until the specimen fails.
2. If the critical level is not reached, the delamination will start but will arrest at a certain length and remain constant at that length (arrest).
3. The stress is so low that delamination never initiates within 500 000 cycles.

In this study, different laminate configurations were tested that included both internal and external ply drops. In addition to this, a thicker material was constructed to represent current industry trends for low-cost, high-volume production of composite structures. For applications, different methods of stopping and arresting delaminations were explored to determine if they were practical solutions to stopping or slowing delaminations.

2. Description of specimens

In this experiment, all the specimens were made using resin transfer molding (RTM) equipment. The plies used in this experiment were made by Knytex in Texas (a wholly-owned subsidiary of Owens/Corning, currently named Owen Corning Fabrics). These plies are made from Owens/Corning E-Glass fibers in various preform configurations. The zero degree layers were D155 material and the $\pm$ 45° layers were DB120. The matrix was a room temperature curing polyester resin manufactured by Interplastic Corporation in Minnesota (CoRezyn 63-AX-051). After the plates were made, 25.4 mm wide specimens were machined and the edges were polished to minimize edge effects from the machining. The coupons were then post cured at 60°C for 2 h. Post-curing assures that the

* Corresponding author.

1359-8368/99/$ - see front matter
PII: S1359-8368(98)00043-2

Table 1
Ply and adhesive material properties

Material	E_{11}	E_{22} (GPa)	E_{33} (GPa)	ν_{12}	ν_{13}	ν_{23}	G_{12} (GPa)	G_{13} (GPa)	G_{23} (GPa)	t (mm)
D155 0° ply[a]	38.4	8.9	8.9	0.29	0.29	0.29	7.4	7.4	4.6	0.45
DB120 (± 45)° ply[a]	11.8	11.8	7.9	0.43	0.28	0.28	7.4	4.1	4.1	0.68
Adhesive[b]	2.6			0.31						

[a] Nominal $V_f = 45\%$
[b] Isotropic

styrene in the polyester has cross-linked to attain maximum composite strength. Nominal material properties may be found in Table 1.

The ply configurations were chosen by selecting the most fatigue resistant material from previous studies [1]. This was the DD5 material with a 38% fiber volume in a $[0/\pm 45/0]_s$ laminate configuration construction using the fabrics as mentioned earlier. The fatigue data for the DD5 material is illustrated in Fig. 1.

3. Static tests

The first test conducted was a static test which was used to determine the critical load for delamination initiation and to determine how a delamination in each configuration would form and grow. Micro-Measurements WK series strain gages were mounted on the thick and thin sections of the coupons to obtain a more accurate measurement of strain than could be obtained by using an extensiometer. The initial tests were the ESA, ESB and ESC laminates. The test matrix was expanded to include such effects as thickness, manufacturing parameters and repair. A guide to all of the laminates is given in Table 2, which contains a list of the laminates tested and the properties of each laminate, including a description. In these initial configurations there was only a single ply drop and the material was the same thickness as the DD5 material. A minimum of five (5) test replicates were used for the studies.

In Fig. 2, it is shown how the laminates behaved, up to delamination initiation. The strain energy release rates (G_c) were determined from the critical load (P_c) using the following strength of materials formula from Ramkumar and Whitcomb [2], and later by Rhee [3].

$$G_c = P_c^2 \frac{A_2E_2 - A_1E_1}{2wA_2E_2A_1E_1} \tag{1}$$

Where: the subscript 1 is for the thin section and 2 is for the thick section of each test coupon, the A is the cross-sectional area and E is Young's modulus, respectively, for each part of the specimen, and w is the width of the coupon.

A diagram of the model used can be seen in Fig. 3. The corresponding nominal critical strain energy release rates for static delamination initiation are 0.12, 1.34 and 1.61 N mm^{-1} for the ESA (single interior ply drop), ESB (interior ply drop of first continuous interior 0° ply), and ESC (center 0° ply drop), respectively. It is interesting to note that the 0° Double Cantilever Beam (DCB) test and the

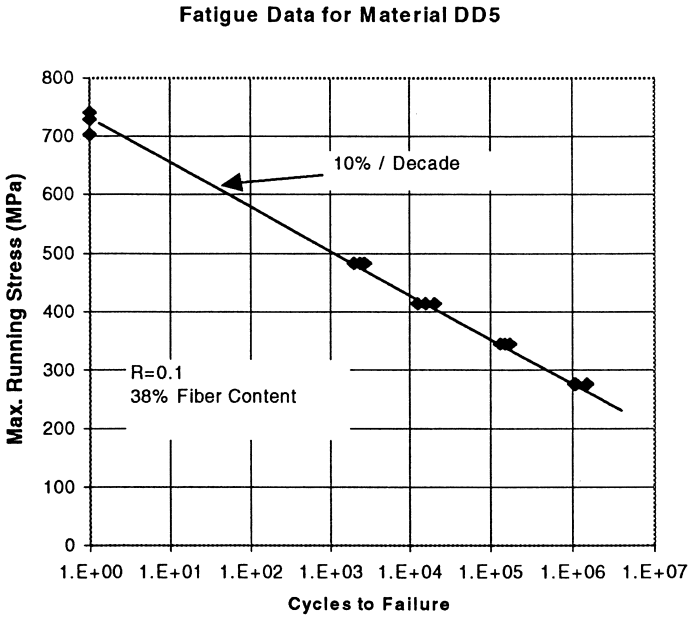

Fig. 1. Fatigue data for DD5 laminate.

Table 2
Laminate configurations, specifications and descriptions

Laminates	Lay-up	E_x (GPa)	V_f (%)	Average thickness (mm), thick/thin	Comments
ESA	$[0^a/(0/\pm 45/0)_s]$	24.0	35.2	3.81/3.10	Single exterior ply drop
ESB	$[0/0^a/\pm 45/0/0/\pm 45/0]$	24.8	35.1	3.7/3.00	Single interior ply drop
ESC	$[0/\pm 45/0/0^a/0\pm 45/0]$	24.3	35.3	3.61/3.02	Single center ply drop
ESE	$[0^a/(0/\pm 45/0)_3]$	30.5	39.7	4.52/3.81	Thicker laminate, single exterior ply drop
ESF	$[0/0^a/\pm 45/0/(0/\pm 45/0)_2]$	33.3	39.7	4.70/4.06	Thicker laminate, single interior ply drop
ESG	$[0^a/0^a/(0/\pm 45/0)_3]$	32.7	38.9	4.95/3.81	Thicker laminate, two exterior ply drops
ESH	$[0/0^a/0^a/\pm 45/0/(0/\pm 45/0)_2]$	34.5	38.9	4.70/3.56	Thicker laminate, two interior ply drops
ESJ	$[0^a/(0/\pm 45/0)_s]$	26.7	37.5	3.56/3.05	Single exterior ply drop, w/'Z-Spiking'
ESK	$[0^a/(0/\pm 45/0)_s]$	29.3	37.4	3.53/2.90	Single exterior ply drop, w/Hysol adhes.

[a] Indicates ply or plies dropped.

End Notched Flexure Test (ENF) tests [4,5] for these same materials are 0.49 and 2.27 N M^{-1}, respectively. All of the laminates are mixed-mode, with the external ply drop more Mode I dominant, and the interior ply drops more Mode II dominant, to be discussed later.

4. Fatigue testing

From the critical loads determined from the static tests, the fatigue load of each laminate could be approximated. All of the tests in this study were run at $R = 0.1$ (minimum/maximum stress) on an Instron 8501 servo-hydraulic testing machine. In the ESA laminate, a single exterior ply was dropped and the initial maximum cyclic stress of 207 MPa in the thin section was chosen. The delamination initiated easily and grew rapidly as can be seen in Fig. 4. It was not until the maximum stress was reduced to 120 MPa (corresponding to approximately 0.5% engineering strain) that the delamination finally arrested after some growth, compared to the static strength of ESA of 452 MPa. The next laminate tested was the ESB laminate which consisted of a single internal ply drop. This laminate schematic can be seen in Fig. 5 later.

From the static testing this laminate had approximately a 68.9 MPa higher stress level before delamination initiation

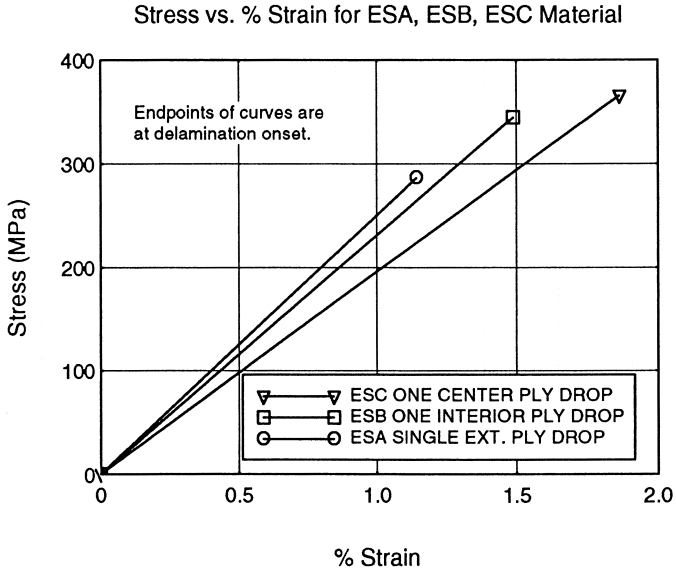

Fig. 2. Stress vs % strain for ESA, ESB, ESC laminates.

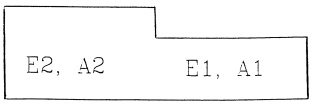

Fig. 3. Model used for G_c calculations.

than the ESA laminate. The internal ply has two shear surfaces to resist delamination and the geometry causes a less severe discontinuity. This was accounted for when calculating the strain energy release rate (G_c) values. Eq. (1) was divided by two to account for the two individual crack fronts, consistent with the strength of materials approach used in its development. The results for the ESB laminate show that the threshold stress for forming delamination (276 MPa) was more than twice as high as for the ESA laminate. Results for the ESC laminate were similar to the ESB laminate, with only a slight gain in the maximum fatigue stress level. The ESC laminate differs from the ESB laminate in that the ply drop is in the center of the laminate rather than immediately under the surface, which reduced the additional bending stress that results as a consequence of asymmetry. From the graphs of the ESB and ESC laminates, delamination resistance in fatigue can be seen in Figs. 6–7, respectively.

To compare the different laminates on the same scale a graph of fatigue delamination growth rate vs normalized energy release rate is given in Fig. 8. This shows that although the strain energy release rate is higher for the ESA than for the ESB laminates, when normalized with their respective G_c, the crack growth rate for both laminates can be correlated with a single relationship. These results are extremely encouraging since they imply that the damage growth rate for different ply drop configurations may be predicted from limited testing on a given material. However, it is noted that the analysis for G_c is based on a strength of materials approach from Eq. (1). This may not be adequate for the complicated mixed mode problem. A nonlinear finite element analysis, as shown in Fig. 9, is currently being used to investigate this problem. It was determined that a nonlinear analysis was necessary because of the membrane/bending coupling in the surrounding plies. This is illustrated by the deformed mesh of Fig. 9. The bridging plies react out the asymmetric loading via bending and membrane stresses and the combination is dependent on the loading. Errors as high as a factor of 2 in G_c calculations can result if the coupling is ignored. Fig. 10 is a detailed closeup of the ESH interior ply drop. From Fig. 10, it is expected that, as a consequence of the geometry, mixed mode fracture occurs in the resin rich region and the subsequent fractured 'window.' To account for different mode types and mixes, the virtual crack closure method described later was used for analysis [6].

5. Virtual crack closure method

A finite element analysis (FEA) model was constructed to examine the initialization, propagation and arrest characteristics of delaminations resulting from plydrops. Three models were developed, each corresponding to ESA, ESB and ESC samples with various delamination lengths. These models used the material and geometric characteristics of the glass/polyester coupons listed in Tables 1 and 2. Both types of plies in the coupons (D155 and DB120) are modeled as 0.508 mm thick. Each plydrop is dropped across a 2.54 mm length. The total model length for all samples is 91.4 mm long with the plydrop starting at 38.1 mm down the length. A two-dimensional plane stress model reduced

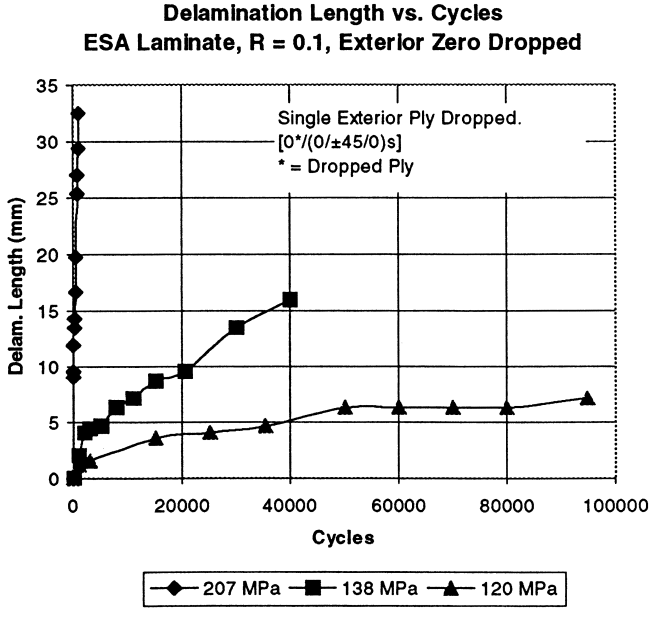

Fig. 4. ESA laminate, delamination rate vs cycles.

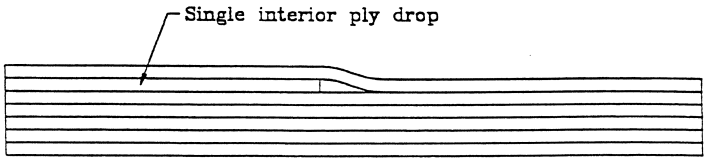

Fig. 5. Sketch of ESB laminate.

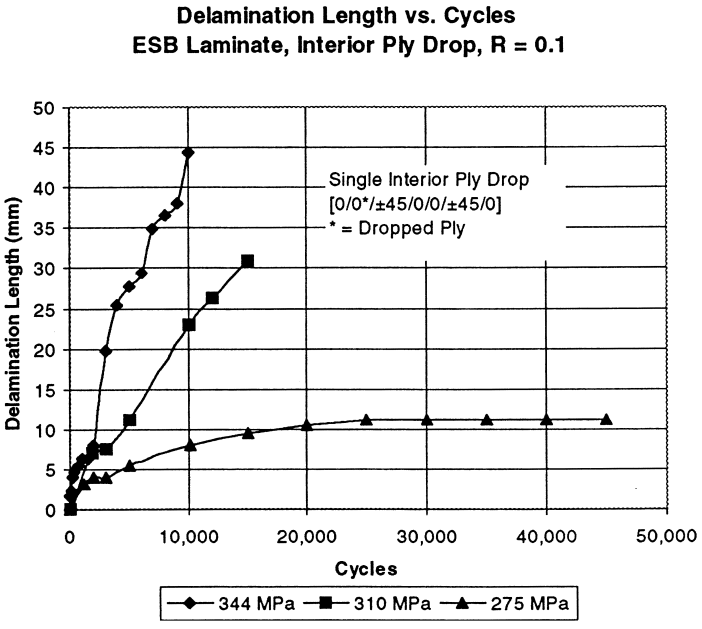

Fig. 6. ESB laminate, delamination rate vs cycles.

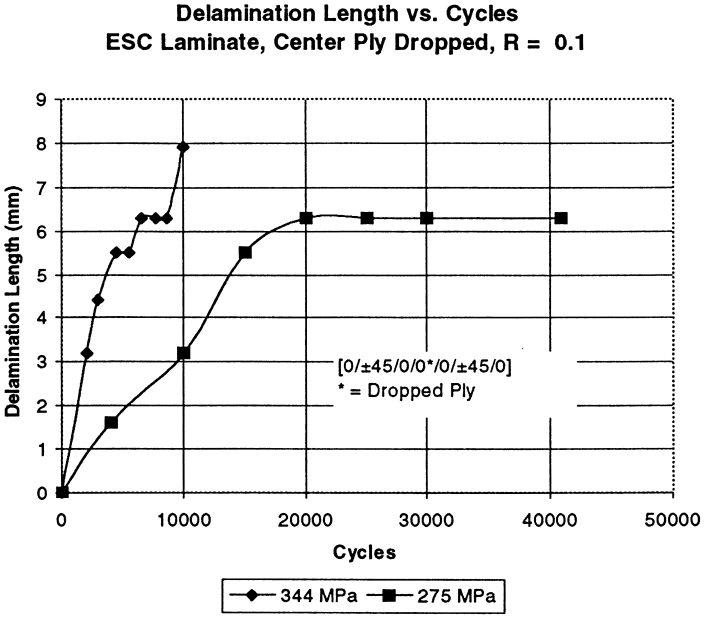

Fig. 7. ESC laminate, delamination rate vs cycles.

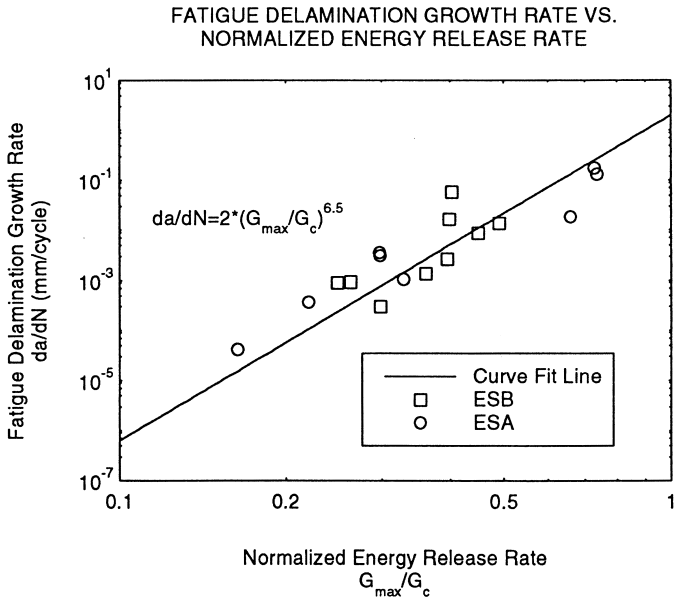

Fig. 8. Fatigue delamination growth rate vs normalized energy release rate.

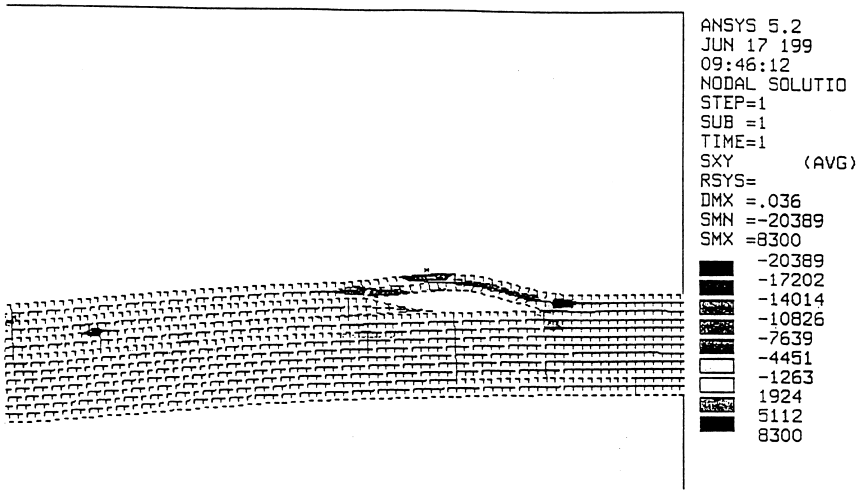

Fig. 9. FEA model of ESB laminate in tension.

the expense involved with a full three-dimensional version. Energy release rates were calculated using the virtual crack closure method, as shown in Eq. (2).

$$G = \frac{1F\Delta u}{2A_c} \tag{2}$$

Where: G is the strain energy release rate for a given mode, F is the force required to close the crack, Δu is the nodal displacement required to close the crack for the given mode, and A_c is the area of the crack closure.

This method allows modal distribution to be analyzed. The method requires the application of virtual loads on nodes closest to the crack front and re-evaluation of the model with these loads. As discussed earlier, it was found that it was necessary to perform a nonlinear analysis for the deformed geometry as shown in Fig. 9 because the membrane stresses contribute to the strain energy distribution. As extension of the laminate occurs, the bridging ply reacts to the asymmetric loading through membrane and bending stresses. At higher strains, the membrane stresses become more important. This is a nonlinear effect. However, the virtual crack closure was found to be linear for the cases considered here. In other words, if there are significant geometric nonlinearities up to the loads of interest, these must be accounted for, but the virtual crack closure can be accomplished by scaling unit loads. By solving for Mode I (opening mode) and Mode II (shear or sliding mode), the total energy release rate can be found. There are currently two schools of thought on how the modal release rates should be added together. One method merely adds them, the second method is the square root of the sum of the squares [7,8].

Table 3
Delamination growth rates for laminates studied (mm/cycle)[a]

Laminate	34.4/344	275/27.5	20.6/206	13.7/137	12.1/121
ESA			1.3×10^{-1}	3.0×10^{-3}	3.8×10^{-4}
ESB	1.4×10^{-2}	9.1×10^{-4}			
ESC	1.1×10^{-3}	2.9×10^{-4}			
ESE			3.0×10^{-2}	1.1×10^{-4}	
ESF			2.1×10^{-3}	4.8×10^{-4}	
ESG				8.6×10^{-4}	2.0×10^{-4}
ESH		1.4×10^{-2}	7.1×10^{-5}		
ESJ		4.4×10^{-3}	4.8×10^{-4}		
ESK			2.8×10^{-3}	1.5×10^{-5}	

[a] Delamination rate (mm/cycle) for Stresses (minimum stress/maximum stress in MPa), $R = 0.1$.

Using the virtual crack closure method, ESA, ESB, and ESC samples were examined for energy release rates from crack initiation and crack arrest using experimental data and loading. Using the accumulated data, it may be possible to predict crack arrest in complex composite structures under fatigue loading. However, it is necessary to first establish a relationship between the energy release rates and the loading before reasonable predictions can be made. Using the virtual crack closure method, in Table 3, the percent of Mode I and II responsible for extending the crack is shown. In this table, the percentage of each mode for the delamination extending into the thicker section (before the ply drop) is given, with the percent strain provided for reference. The analyses were conduced at the experimentally-measured arrest damage sizes. Most of the initiation (small crack lengths), was dominated by Mode I crack growth. The crack also extended into the thinner section (after the ply drop), the corresponding percentages are given in Table 4.

For this purpose, it is expedient to establish a larger database of energy release rates from the virtual crack closure models to compare with experimental data. Of particular note, as the crack grows, the fracture is dominated by Mode II strain energy release rates. Hence, initiation appears to occur in the detailed, resin-rich area in Mode I, and progresses to Mode II domination.

6. Laminates ESE, ESF, ESG and ESH

After the first three laminates were studied, it was decided that other laminate configurations should be considered. The ESE and ESF laminates were thicker laminates with a single ply drop. The ESE laminate had an exterior ply drop while the ESF laminate had an interior ply drop.

The ESE laminate had a lower delamination growth rate than the ESA laminate, which had a smaller overall cross-sectional area. The G_c for both the ESA and ESE laminates, along with the ESF laminate compared with the ESB laminate were similar.

The ESG and ESH laminate were also thicker in cross-section, but, in an attempt to simulate a potential manufacturing situation, two plies were dropped at a single location instead of one ply. The ESG laminate contained two ply drops on the outside while the ESH laminate contained two ply drops on the interior. In both cases, these configurations behaved poorly compared with their single ply drop counterparts. During testing of the ESH laminate, the resin rich area ahead of the ply drop was observed to fragment during the fatigue test. When the coupon was in the maximum stress part of the fatigue cycle a fracture in the resin pocket through the laminates width was seen. No material was left ahead of the ply drop after the first initial cycles. This is illustrated in Fig. 10 and described as the 'window' in this region.

The ESG laminate with a double external ply drop delaminated more easily than a single ply drop on the outside. One apparent reason for this is the higher critical strain energy release rate of the ESA laminate, the G_c of the ESG laminate was only 1.26 N mm^{-1}, while the G_c for the ESA laminate was 1.89 N mm^{-1}. Another reason for this was the increased bending moment created by the eccentricity of having two layers creating the ply drop, as well as the larger dropped area. A comparison of laminates which

Table 4
Percentage of strain energy release rates for crack growth into thicker section[a]

Laminate	Percent Mode I (opening)	Percent Mode II (shearing)
ESA(0.46% strain)	40.7	59.3
ESB(1.06% strain)	—	100
ESC(1.07% strain)	—	100

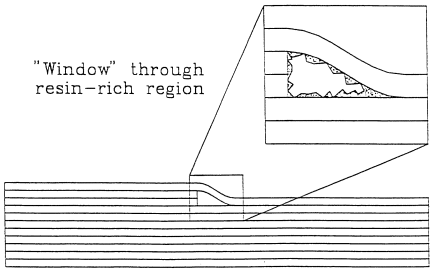

Fig. 10. Sketch of resin rich region in ESH laminate.

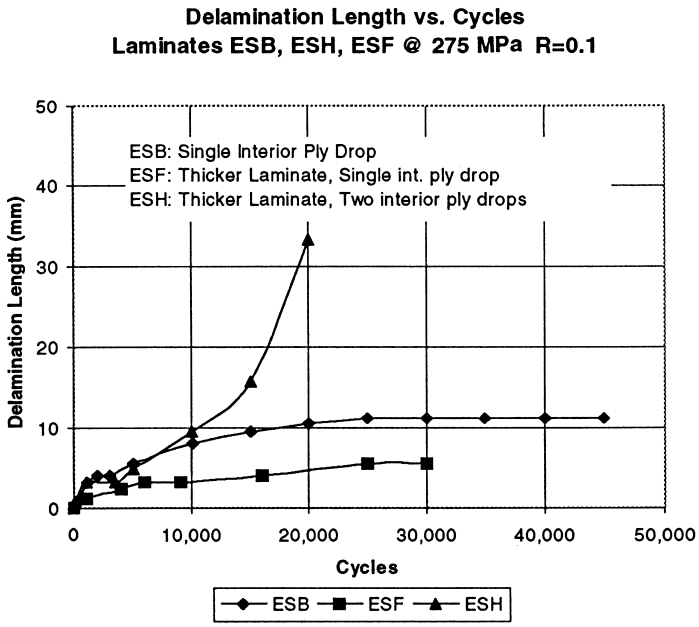

Fig. 11. Comparison of internal ply drops at 275 MPa.

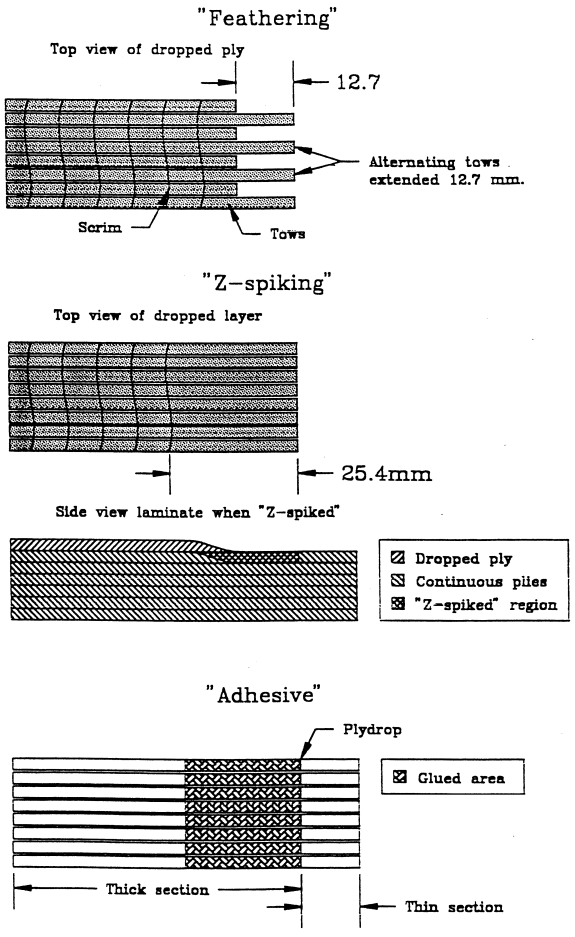

Fig. 12. Illustrations of feathering, 'Z-Spiking', an using Hysol adhesive to prevent delamination.

contained internal ply drops is presented in Fig. 11. As noted earlier, the ESH laminate with two interior ply drops had the highest delamination growth rate. The best configuration was the ESF laminate, which was a thicker laminate with a single internal ply drop. This laminate has less bending stresses and better surrounding material load carrying capability than the comparable ESB and ESC laminates.

7. Attempt at improving delamination resistance

After the previous configurations were tested, methods of preventing delamination were studied. The first configuration used the ESA laminate as a basis for comparison and a second configuration used the ESB laminate as a basis. First, random mat fabric was included between the ply drop and the first continuous zero layer. A second modification is called 'feathering'. In this case, alternating tows were pulled approximately 13 mm past the adjacent tows to provide a less defined ply drop front and delamination site (Fig. 12).

In two other cases, the ESJ and ESK laminates, innovative methods were used to prevent delamination (Fig. 12). In the ESJ laminate, 'Z-Spiking' was used, which consisted of removing the binder from the fabric and driving the fiber tows into the lower layers. The transverse strength properties are much lower than the longitudinal properties, providing fiber reinforcement in the thickness direction results in additional resistance to delamination. The ESK laminate used a 25 mm wide layer of Hysol EA 9309.2NA adhesive approximately 0.3 mm thick, between the outer ply drop and the first continuous zero layer. This adhesive was applied and was allowed to cure before the resin was injected into the mold. The theory behind this attempt was that by

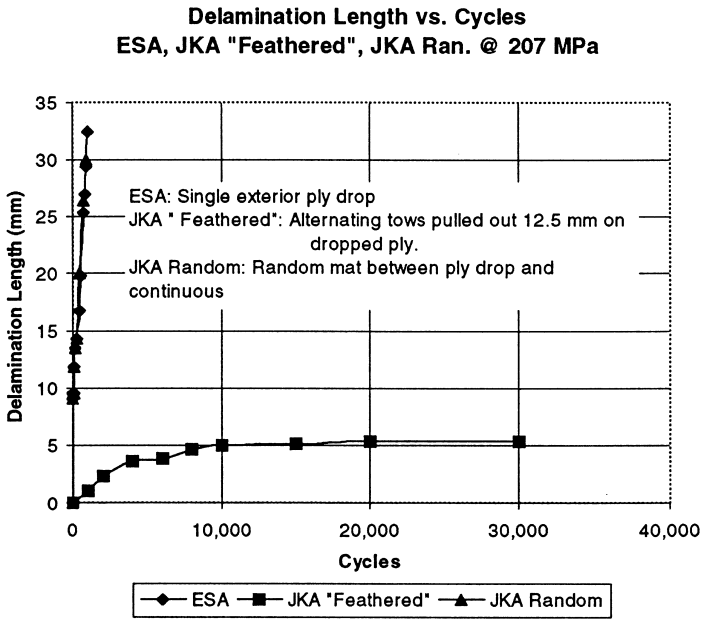

Fig. 13. Comparison of ESA, JKA 'feathered', JKA random at 207 MPa.

applying a thin, tough adhesive, delamination initiation would be resisted. Also the adhesive layer enhances the process zone for fracture [9,10]. It is noted that 'Z-Spiking' and adding local adhesive can also easily be applied in a hand lay-up manufacturing process as well.

8. Results from delamination prevention techniques

Since all of the delamination prevention techniques were applied to the same layer configuration as the ESA laminate, the ESA laminate was used as a standard by which the other laminates were judged. As can be seen from Fig. 13, the feathered laminate provided a substantial decrease in the delamination growth rate. However, applying random mat to the lay-up had little effect and possibly increased the delamination growth rate. An extensive study was not performed here, but this result is consistent with other studies, wherein if the process zone in the interply region is suppressed with reinforcement, the critical strain energy release rate decreases [9].

In Fig. 14, the ESK laminate with the Hysol adhesive is compared with three other laminates. The ESK laminate demonstrated a significant improvement over the other

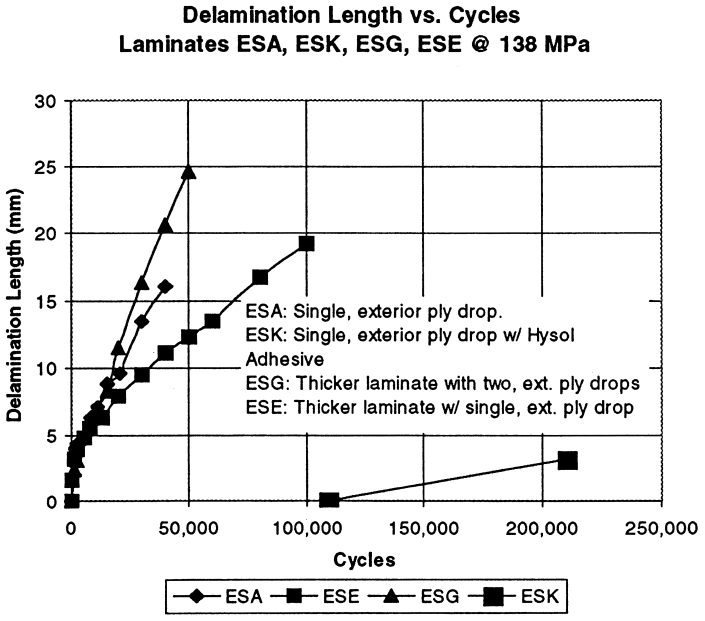

Fig. 14. Comparison of exterior ply drop configurations at 138 MPa.

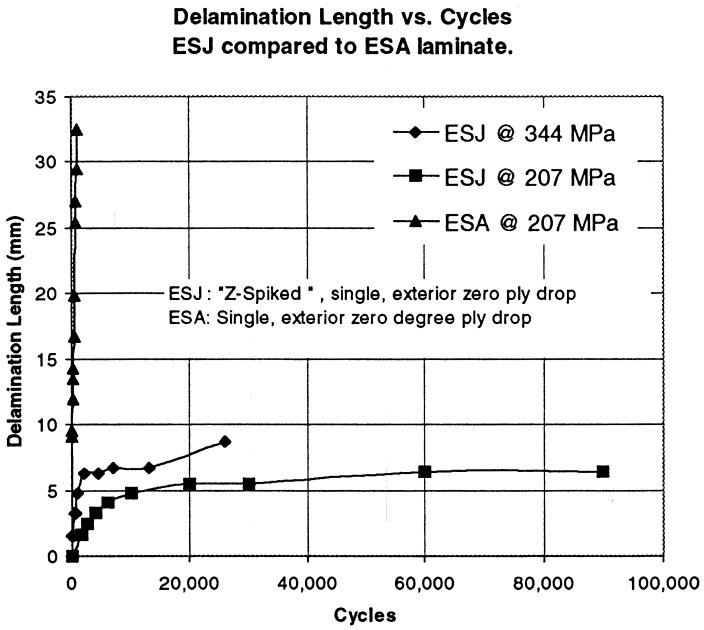

Fig. 15. ESA vs ESJ 'Z-Spiked' laminate.

configurations tested. The delamination in the ESK laminate did not initiate until the other laminates had completely delaminated. The ESJ laminate with 'Z-Spiking' is not shown on this graph because there was no delamination initiation in more than 200 000 cycles at the same stress level. Both 'Z-spiking' and the Hysol adhesive delamination did not initiate like the other laminates. In both cases, the delamination initiated at the specimen edges, as expected from previous studies [11–13]. These edge delaminations occurred even though the edges of the specimens were carefully polished. Polishing mitigates, but does not preclude free-edge effects. The results for the ESJ laminate are illustrated in Fig. 15. Note that 'Z-spiking' has a profound influence on the arrest, presumably resulting from the extensive fiber bridging noted in these samples. The ESB laminate results, with feathered ply drops, are presented in Fig. 16. From Fig. 16, it can be clearly seen for the ESB laminate with feathered ply drops that the delamination started but stopped, while the ESB material with no feathering continued to grow until arrest at a much larger delamination length. In Table 2, the delamination rate for various stress levels and laminates ESA through ESK is

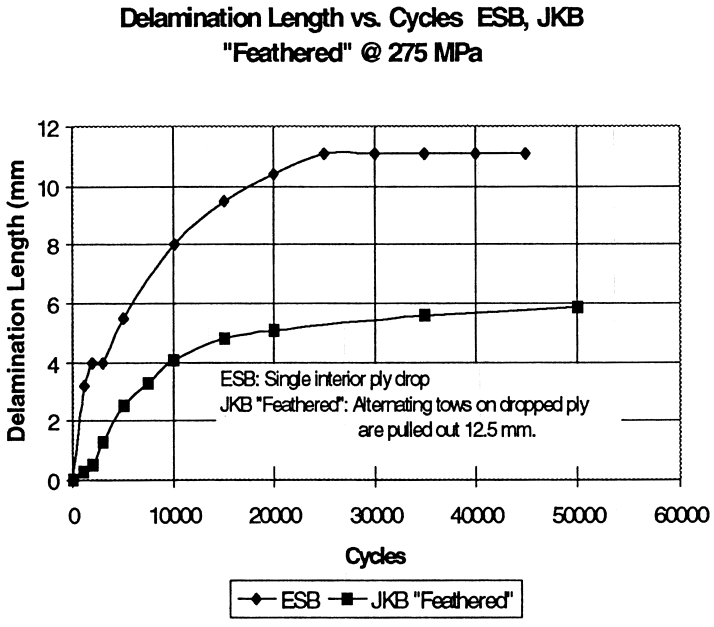

Fig. 16. ESB vs JKB 'feathered' at 275 MPa.

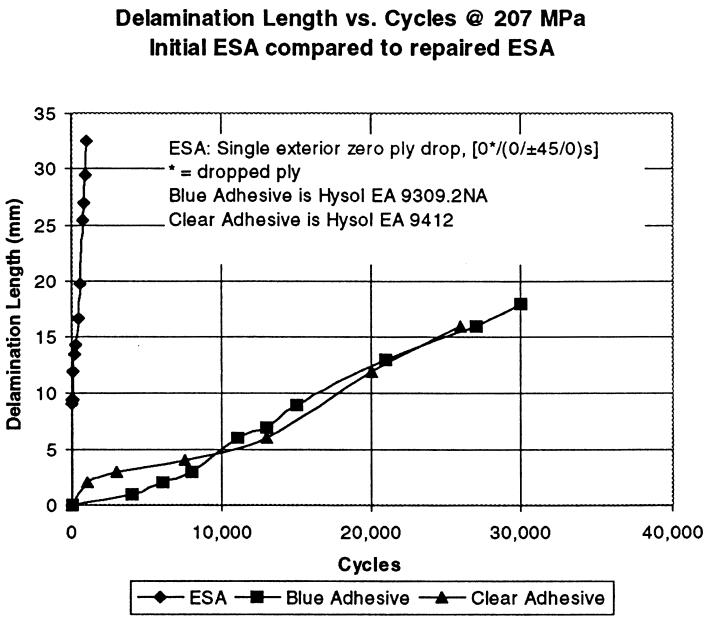

Fig. 17. Initial ESA vs repaired ESA at 206 MPa.

presented. In this table, the *R* ratio (min stress/max stress) value equals 0.1.

9. Repairing samples previously tested

During testing the ESA laminate, which had an exterior ply drop, the outer layer peeled away from the rest of the laminate. For practical purposes, it was desired to determine whether it is possible to repair the delamination with two epoxy adhesives. The first adhesive was Hysol EA 9309.2NA, which is blue in color, while the second one was Hysol EA 9412, which is clear. After the initial test run, the adhesive was injected into the delamination via syringe. A C-clamp was applied to the specimen until the adhesive cured. These procedures were adopted to simulate practical field repairs for composite structures. The specimen was then retested at the same stress level and the delamination growth rate was compared to the original rate, which can be seen in Fig. 17. From Fig. 17, the two adhesives had a similar delamination growth rate and provided a significant reduction in delamination growth rate compared with the original laminate.

10. Conclusions and design recommendations

From the foregoing results, the following general conclusions can be drawn about delamination and delamination prevention:

1. For the same ply drops, thicker laminates are better in resisting delamination.
2. Dropping more than one ply at the same location increases the delamination growth rate.
3. Internal ply drops are more resistant to delamination than external ply drops.
4. Repairing external plies using an adhesive is effective in preventing delamination from starting again.
5. The use of ‘Z-Spiking’ and adhesives in the initial manufacturing of parts with ply drops substantially reduces the initial delamination growth rate.
6. Using feathering at the ply drops reduces the delamination growth rate.
7. Random mat possibly has a detrimental effect on delamination resistance.

On the basis of these results, an optimum configuration of dropping plies may be to have an internal ply drop, with a combination of either ‘Z-Spiking,’ an adhesive or ‘feathering’ used in the construction.

11. Further study

The current analysis for ply drops is based on a strength of materials approach. it is encouraging that this approach may be adequate for damage growth during fatigue as was shown in Fig. 8. This warrants additional studies. The strength of materials approach does not include details at the crack tip region. Further studies will incorporate more

Table 5
Percentage of strain energy release rates for crack growth into thinner section[a]

Laminate	Percent Mode I (opening)	Percent Mode II (shearing)
ESB (1.06% strain)	73.8	26.2
ESC (1.07% strain)	38.6	61.4

detailed analyses, including the fracture mode type and the fracture mode mix to expand on some of the interesting results of Tables 2–5. This may explain some of the differences in G_c for the various laminates. In particular, the discrepancies between the DCB and ENF tests need to be explored.

In the future, determining the effect of spacing of ply drops should be considered. By doing this the number of plies that can be dropped over a given length can be determined. If the ply drops are too close together, then a resin rich area could possibly form, leading to failure (as in the ESH laminate). However, if the ply drops are too far apart, then tapering the thickness may be too gradual and therefore, non-optimal.

Acknowledgements

This work was supported by the US Department of Energy and the State of Montana through the Montana DOE EPSCoR Program (contract # DE-FC02-91ER75681) and NREL (contract # XF-1-11009-5).

References

[1] Samborsky DD, Mandell JF. Fatigue resistant fiberglass laminates for wind turbine blades. In: ASME Wind Symposium, Houston, TX, 1996.

[2] Ramkumar RL, Whitcomb JD. Characterization of Mode I and mixed-mode delamination growth in T300/5208 graphite/epoxy, in delamination and debonding of materials. In: Johnson WS, editor. ASTM STP 876. Philadelphia, PA: American Society for Testing and Materials, ASTM, 1985:315–335.

[3] Rhee KY. Characterization of delamination behavior of unidirectional graphite/PEEK laminates using cracked lap shear (CLS) specimens. Composite Structures 1994;29:379–382.

[4] Whitney JM, Browning CE, Hoogsteden W. A double cantilever beam test for characterizing mode i delamination in composites. Journal of Reinforced Plastics and Composites 1982;1:297.

[5] Carlsson LA, Gillespie Jr. JW. On the design and analysis of end notched flexure (ENF) specimen for Mode II testing. Journal of Composite Materials 1986;20.

[6] Rybicki EF, Kanninen MF. A finite element calculation of stress-intensity factors by a modified crack closure integral. Engineering Fracture mechanics 1977;9:931–938.

[7] Gong Xiao-Jing, Benzeggagh Malk. Mixed mode interlaminar fracture toughness of unidirectional glass/epoxy composites. In: Martin RH, editor. Composite Materials: Fatigue and Fracture — Fifth Volume, ASTM STP 1230. Philadelphia, PA: American Society for Testing and Materials, 1995:100–123.

[8] O'Brien TK. Characterization of delamination onset and growth in a composite laminate. In: Reifsnider KL, editor. Damage in Composite Materials, ASTM STP 775. Philadelphia, PA: American Society for Testing and Materials, 1982.

[9] Cairns DS. Prediction of fracture toughness of multi-phase materials. In: Proceedings of the AIAA/ASME/ASCE/AHS/ASC 31st Structures, Structural Dynamics and Materials Conference, April 1990.

[10] Cairns DS. Mixed-mode fracture and toughening in multi-phase materials. In: Proceedings of the ASCE Engineering Mechanics Speciality Conference, 20–22 May 1991.

[11] Wang AS, Crossman FW. Initiation and growth of transverse cracks and edge delamination in composite laminates — Part 1: an energy method. Journal of Composite Materials 1980;14(1):71–87.

[12] Chan WS, Wang ASD. Free edge delamination characteristics in S2/CE9000 glass/epoxy laminates under static and fatigue loads. In: Composite Materials Fatigue and Fracture, ASTM STP 1012. Philadelphia, PA: American Society for Testing and Materials, 1989:270–295.

[13] Allix O, Gornet L, Ladeveze P, Leveque D, Delamination prediction by continuum damage mechanics.In: Proceedings of the IUTAM Symposium — Variations of Domains and Free-boundary problems, 22–25 April. Paris, France: Kluwer Academic Publishers, 1997.